Chiral approach to antikaon s- and p-wave interactions in dense nuclear matter

L. Tolós
Gesellschaft für Schwerionenforschung,
Planckstrasse 1, D-64291 Darmstadt, Germany

A. Ramos
Departament d'Estructura i Constituents de la Matèria,
Universitat de Barcelona, Diagonal 647, 08028 Barcelona, Spain

E. Oset
Departamento de Física Teórica and IFIC,
Centro Mixto Universidad de Valencia-CSIC,
Institutos de Investigación de Paterna,
Ap. Correos 22085,
E-46071 Valencia, Spain

(Dated: July 23, 2013)

Abstract

The properties of the antikaons in nuclear matter are investigated from a chiral unitary approach which incorporates the s- and p-waves of the $\bar{K}N$ interaction. To obtain the in-medium meson-baryon amplitudes we include, in a self-consistent way, Pauli blocking effects, meson self-energies corrected by nuclear short-range correlations and baryon binding potentials. We pay special attention to investigating the validity of the on-shell factorization, showing that it cannot be applied in the evaluation of the in-medium corrections to the p-wave amplitudes. In nuclear matter at saturation energy, the Λ and Σ develop an attractive potential of about -30 MeV, while the Σ^* pole remains at the free space value although its width gets sensibly increased to about 80 MeV. The antikaon also develops a moderate attraction that does not support the existence of very deep and narrow bound states, confirming the findings of previous self-consistent calculations.

PACS numbers: 13.75.-n; 13.75.Jz; 14.20.Jn; 14.40.Aq; 21.65.+f; 25.80.Nv

I. INTRODUCTION

The interaction of $\bar{K}$ with nucleons and nuclei has captured much interest in recent times [1]. The elementary interaction close to threshold is linked to the presence below threshold of the $\Lambda(1405)$ resonance, long claimed to be a dynamically generated resonance in coupled channels [2, 3] more than a genuine three constituent quark state. The advent of chiral theories [4–8] and unitarization extensions in coupled channels has brought a new perspective into the topic and reconfirmed these first claims [9–13]. It has also allowed to tackle the problem in a more systematic way and has brought some surprises, as the existence of more dynamically generated resonances like the $\Lambda(1670)$ [14–16], the $\Xi(1620)$ [17], the $\Xi(1690)$ [18], hints of some resonance in $I = 1$ and $S = -1$ in [11], etc. A thorough work, looking at the SU(3) group structure of the generated states, has allowed a generalization of the problem concluding that there is a singlet and two octets of states which are dynamically generated in the interaction of the octet of pseudoscalar mesons with the octet of $1/2^+$ baryons [16, 18]. There is also a surprise in this investigation which concludes that the actual experimental $\Lambda(1405)$ is a superposition of two states and that this should have experimental repercussions by making the $\Lambda(1405)$ appear with different energy and width in different reactions. This claim had a recent experimental confirmation in the experiment of [19] and the posterior analysis of the experiment in [20].

The interaction of $\bar{K}$ in nuclei has had a parallel and equally exciting development. The K^-N scattering matrix at threshold is repulsive. However, the phenomenology of kaonic atoms demands an attractive potential [21, 22], which is telling us that, in spite of the small nuclear densities experienced by the K^- atoms, the low density theorem $\Pi = t\rho$, where Π is the K^- self-energy ($2\omega V_{\rm opt}$), t the scattering matrix and ρ the nuclear density, breaks down already at these small densities. The presence of the $\Lambda(1405)$ resonance just below $\bar{K}N$ threshold is at the root of this problem. The first step to understand this change of sign was given in [23] (see also [24]) which showed that the consideration of Pauli blocking in the intermediate $\bar{K}N$ states moved the position of the $\Lambda(1405)$ resonance, or, equivalently, the zero of the real part of the $\bar{K}N$ amplitude, to higher energies, hence passing from a free-space repulsive scattering matrix at threshold to an attractive one in the medium. The problem is more subtle, as was shown in [25] (see also [26]), since the self-consistent consideration of the generated attractive self-energy in the $\bar{K}$ has as a consequence the shift of the resonance position to lower energies introducing a repulsion. The final self-consistent solution still leads to a moderate attraction on the $\bar{K}$, but much smaller than by just considering the Pauli blocking effect. A further consideration of the self-energies of the pions and baryons in the intermediate states was done in [27] opening new decay channels for the $\bar{K}$ but not modifying much the real part of the potential. Moderate attractions of the order of -50 MeV at full nuclear matter density are found in these approaches and the potential obtained is shown to fairly reproduce the data on kaonic atoms [28]. This fairness is further investigated in [22] where a fit to data is made in order to see how far is the calculated potential from an optimal one. The potential of [27] also leads to deeply bound K^- states in medium and heavy nuclei which are bound by about 30-40 MeV but have a width of about 100 MeV [28].

Different steps in this problem were given in [29], constructing a kaon-nucleus potential with very large strength and predicting strongly bound states in few body systems. This phenomenological potential has been critically discussed in [30], where it is shown that the omission of the direct coupling of the $\pi\Sigma$ channel to itself, the assumption of the nominal $\Lambda(1405)$ as a single bound $\bar{K}$ state –while there are two states in the chiral unitary approach– , the lack of self-consistency in the calculations and the seemingly too large nuclear densities obtained of around ten times normal nuclear matter density at the center of the nucleus, lead altogether to a much larger potential than that obtained in the chiral approaches. With the potential of [29] a bound state of K^- in ^{3}He by 108 MeV was predicted in $I = 0$. Later on an experiment at KEK found a peak in the proton spectrum following the absorption of stopped K^- by ^{4}He [31], which was interpreted as a strange tribaryon with $I = 1$, and not as a kaon atom, since its interpretation as a kaon atom required 195 MeV binding and the isospin was also different than the predictions made in [29]. However, further work done in [32] including relativistic corrections (always considered in the chiral approaches), spin orbit effects and some further ad hoc changes produced a binding in the three body system compatible with the association of the tribaryon state claimed in [31] to the kaon bound state. At this point the K^--nucleus potential has a strength of 615 MeV at the center of the nucleus, roughly twenty times what one would get from the chiral theories for this problem. Such disparate approaches led the authors of [30] to search for a different interpretation of the peaks found in the experiment of [31], and an explanation of the peaks was found based on the mechanism of K^- absorption in nucleon pairs leading to Λp and Σp without further interaction of the final pair of particles with the nucleus.

Another experiment, looking at the Λp invariant mass after K^- absorption in different light and medium nuclei, interpreted a broad peak as a bound state of K^-pp by 115 MeV [33]. Such a large number and the alternative explanation found for the KEK peaks, motivated the authors of [34] to look for another interpretation of the peak, which was found in the process of K^- absorption by pairs of nucleons leading to ΛN, followed by the scattering of the Λ or the N with the daughter nucleus.

On the theoretical side there have been further advances by looking at the p-wave contribution to the optical potential [35–37]. In [35] the p-wave K^--nucleus optical potential was studied for atoms and found to be basically negligible. Yet, for other situations where the momenta of the kaon could be larger than in the atoms, this contribution could be bigger and it is thus mandatory to address this problem. Some work in this direction has already been done in [36], where the momentum dependence of the antikaon potential in nuclear matter was obtained from a self-consistent calculation using the meson-exchange Jülich interaction. At momenta as large as 500 MeV/c, the higher partial waves beyond $L = 0$ modify strongly the $\bar{K}$ potential.

In view of the interest and controversy of the subject, the importance of having an accurate as possible description of the interaction of $\bar{K}$ with nucleons in nuclear matter is rather evident and it is our purpose to present here the results of a careful study of the s- and p-wave contributions to the $\bar{K}$ nucleus potential. The work follows closely the lines

of [27], incorporating the many-body corrections to the p-wave $\bar{K}N$ interaction studied in [38] within the same chiral unitary approach. An evaluation of the antikaon propagation in matter based on chiral dynamics including s-, p- and d-waves was already performed in [37]. We will investigate the validity of the on-shell factorization of the kernel in the Bethe-Salpeter equation. This approach is often used in the study of the hadron-hadron collisions and finds its justification in the N/D dispersion relation method used in [11] and [39]. However, this is not justified when one goes to the nuclear medium since there are new sources of imaginary part different from those of the free case. As we shall see, the use of this prescription in the nuclear medium for p-waves leads to a violation of causality, producing negative decay widths in some cases. A different sort of on-shell aproximation is done in Ref. [37], which in practice leads to quite diferent results for p-waves than those reported here.

A byproduct of any calculation including a self-consistent propagation of p-waves in a coupled-channel scheme is the self-energy of the hyperons involved in the p-wave $\bar{K}N$ interaction kernel. At variance to Ref. [37], the in-medium $\bar{K}N$ amplitudes calculated in the present work include self-energy insertions not only on the antikaons but also on the pions present as intermediate states in the coupled-channel scheme. This gives rise to a more realistic derivation of the hyperon self-energies, as we shall see, since important YN interaction pieces, such as $\Lambda N \to \Sigma N$, conveniently modified by the effect of short-range correlations are also included in the present work.

The paper is organized as follows. We first recall in Sect. II the structure of the s- and p-wave $\bar{K}N$ amplitudes in free space. Next, in Sect. III, we describe how the different medium effects are incorporated into our scheme, paying special attention to discussing the validity of the on-shell factorization in the medium as well as to showing how the intermediate meson propagators get modified by the effect of short-range correlations. In Sect. IV we present and discuss our results for the in-medium amplitudes and the antikaon properties, such as the spectral function or the optical potential. Finally, our concluding remarks are given in Sect. V.

II. MESON-BARYON AMPLITUDES IN FREE SPACE

The lowest order chiral Lagrangian which couples the octet of pseudoscalar mesons to the octet of $1/2^+$ baryons is given by [5–8]

$$\begin{aligned}\mathcal{L}_1^{(B)} &= \langle \bar{B} i\gamma^\mu \nabla_\mu B\rangle - M\langle \bar{B}B\rangle \\ &\quad + \frac{1}{2}D\left\langle \bar{B}\gamma^\mu\gamma_5\left\{u_\mu, B\right\}\right\rangle + \frac{1}{2}F\left\langle \bar{B}\gamma^\mu\gamma_5\left[u_\mu, B\right]\right\rangle \ , \end{aligned} \tag{1}$$

where B is the SU(3) matrix for baryons, M is the baryon mass, u contains the Φ matrix of mesons and the symbol $\langle\,\rangle$ denotes the trace of SU(3) flavor matrices. The SU(3) matrices appearing in Eq. (1) are standard and can be seen in the former references. The couplings D and F are chosen as $D = 0.85$ and $F = 0.52$.

At lowest order, the $BB\Phi\Phi$ interaction Lagrangian reads

$$\mathcal{L}_1^{(B)} = \left\langle \bar{B} i\gamma^\mu \frac{1}{4f^2}[(\Phi\,\partial_\mu\Phi - \partial_\mu\Phi\Phi)B - B(\Phi\,\partial_\mu\Phi - \partial_\mu\Phi\Phi)] \right\rangle \ . \tag{2}$$

For low energies, one derives the s-wave amplitude

$$V_{ij}^s = -C_{ij}\,\frac{1}{4f^2}\,(2\,\sqrt{s} - M_{B_i} - M_{B_j})\left(\frac{M_{B_i}+E_i}{2\,M_{B_i}}\right)^{1/2}\left(\frac{M_{B_j}+E_j}{2\,M_{B_j}}\right)^{1/2} \ , \tag{3}$$

being M_{B_i} and E_i the mass and energy of the baryon in the i channel, respectively. The coefficients C_{ij} form a symmetric matrix and are written explicitly in [10]. Following Ref. [10], the meson decay constant f is taken as an average value $f = 1.123 f_\pi$ [14]. The channels included in our study are K^-p, $\bar{K}^0n$, $\pi^0\Lambda$, $\pi^0\Sigma^0$, $\eta\Lambda$, $\eta\Sigma^0$, $\pi^+\Sigma^-$, $\pi^-\Sigma^+$, $K^+\Xi^-$, $K^0\Xi^0$. We note, for later purposes, that this equation can be written to a good approximation as

$$V_{ij}^s \simeq -C_{ij}\,\frac{1}{4f^2}\,(k_j^0 + k_i^0) \ , \tag{4}$$

where k_i^0 and k_j^0 are the initial and final meson energies in the center-of-mass (c.m.) frame. The lagrangian in Eq. (2) provides also a small part of the p-wave, which in the c.m. frame reads:

$$V_{ij}^c = -C_{ij}\frac{1}{4f^2}\,a_i\,a_j\left(\frac{1}{b_i}+\frac{1}{b_j}\right)(\vec{\sigma}\cdot\vec{q}_j)(\vec{\sigma}\cdot\vec{q}_i) \ , \tag{5}$$

with

$$a_i = \sqrt{\frac{E_i+M_i}{2M_i}} \ , \qquad b_i = E_i + M_i \ , \qquad E_i = \sqrt{M_i^2 + \vec{q}_i^{\,2}} \ . \tag{6}$$

The main contribution to the p-wave amplitude comes from the Λ and Σ pole terms which are obtained from the D and F terms of the Lagrangian of Eq. (1) [38]. The Σ^* pole term is also included explicitly with couplings to the meson-baryon states evaluated using SU(6) symmetry arguments [40]. These contributions are given by:

$$\begin{aligned}
V_{ij}^\Lambda &= D_i^\Lambda D_j^\Lambda \frac{1}{\sqrt{s}-\tilde{M}_\Lambda}(\vec{\sigma}\cdot\vec{q}_j)(\vec{\sigma}\cdot\vec{q}_i)\left(1+\frac{q_j^0}{M_j}\right)\left(1+\frac{q_i^0}{M_i}\right) \ , \\
V_{ij}^\Sigma &= D_i^\Sigma D_j^\Sigma \frac{1}{\sqrt{s}-\tilde{M}_\Sigma}(\vec{\sigma}\cdot\vec{q}_j)(\vec{\sigma}\cdot\vec{q}_i)\left(1+\frac{q_j^0}{M_j}\right)\left(1+\frac{q_i^0}{M_i}\right) \ , \\
V_{ij}^{\Sigma^*} &= D_i^{\Sigma^*} D_j^{\Sigma^*} \frac{1}{\sqrt{s}-\tilde{M}_{\Sigma^*}}(\vec{S}\cdot\vec{q}_j)(\vec{S}^\dagger\cdot\vec{q}_i) \ ,
\end{aligned} \tag{7}$$

with $S^\dagger$ being the spin transition operator from spin 1/2 to spin 3/2 and

$$\begin{aligned}
D_i^\Lambda &= c_i^{D,\Lambda}\sqrt{\frac{20}{3}}\frac{D}{2f} - c_i^{F,\Lambda}\sqrt{12}\frac{F}{2f} \ , \\
D_i^\Sigma &= c_i^{D,\Sigma}\sqrt{\frac{20}{3}}\frac{D}{2f} - c_i^{F,\Sigma}\sqrt{12}\frac{F}{2f} \ , \\
D_i^{\Sigma^*} &= c_i^{S,\Sigma^*}\frac{12}{5}\frac{D+F}{2f} \ .
\end{aligned} \tag{8}$$

The constants c^D, c^F, c^S are SU(3) Clebsch-Gordan coefficients which depend upon the meson and baryon involved in the vertex and are given in Table I of Ref. [38]. The masses $\tilde{M}_\Lambda$, $\tilde{M}_\Sigma$, $\tilde{M}_{\Sigma^*}$ are bare masses of the hyperons ($\tilde{M}_\Lambda$=1030 MeV, $\tilde{M}_\Sigma$=1120 MeV, $\tilde{M}_{\Sigma^*}$=1371 MeV), which will turn into physical masses upon unitarization.

Once the tree level contributions to the s- and p-wave meson-baryon scattering are known, the Bethe-Salpeter equation can be solved using the tree level contributions as the kernel of the equation. In Ref. [10] it was shown that the kernel for the s-wave amplitude can be factorized on the mass shell in the loop functions, by making some approximations typical of heavy-baryon perturbation theory. Then the Bethe-Salpeter equation turns out to be simpler to solve. Furthermore, the factorization for p-waves in meson-meson scattering is also proved in [41] along the same lines. A more general proof of the factorization is done in [39] for meson-meson interactions and in [11] for meson-baryon ones.

The formal result obtained is schematically given by

$$T = V + VGT, \tag{9}$$

that is

$$T = [1 - VG]^{-1}V \ , \tag{10}$$

where V is the kernel (potential), given by the s- and p-wave amplitudes of Eqs. (3),(5),(7), and G is a diagonal matrix accounting for the loop function of a meson-baryon propagator, which needs to be regularized. This can be done by adopting either a cut-off method or by using dimensional regularization. The cut-off method is easier and more transparent when dealing with particles in the medium as it will be our case. The use of this cut-off scheme or the dimensional regularization are in practice identical, given the matching between the two loop functions done in Section 2 of Appendix A of Ref. [42]. There, one finds that the dimensional regularization formula and the one with cut-off have the same analytical properties (the log-terms) and are numerically equivalent for values of the cut-off reasonably larger than the on-shell momentum of the states in the loop, which is a condition respected in our calculations. By fine tuning the subtraction constant in dimensional regularization, or fine tuning the cut-off, one can make the two expressions identical at one energy and practically equal in a wide range of energies, sufficient for studies like the present one. Using the cut-off regularization the loop function reads in the c.m. frame

$$\begin{aligned} G_l(\sqrt{s}) &= i \int \frac{d^4q}{(2\pi)^4} \frac{M_l}{E_l(-\vec{q})} \frac{1}{\sqrt{s} - q^0 - E_l(-\vec{q}) + i\epsilon} \frac{1}{q^2 - m_l^2 + i\epsilon} \\ &= \int_{|\vec{q}|<q_{\rm max}} \frac{d^3q}{(2\pi)^3} \frac{1}{2\omega_l(\vec{q})} \frac{M_l}{E_l(-\vec{q})} \frac{1}{\sqrt{s} - \omega_l(\vec{q}) - E_l(-\vec{q}) + i\epsilon} \, , \end{aligned} \tag{11}$$

with $\sqrt{s} = k^0 + p^0$, being $p^0(k^0)$ the energy of the initial baryon (meson) and $q_{\rm max} = 630$ MeV.

The p-wave amplitudes of Eqs. (5),(7) cannot be used directly in Eq. (10) since, due to their spin structure, there is a mixture of different angular momenta. As done in Ref. [38],

we separate the p-wave amplitudes according to the total angular momentum. With the partial-wave amplitude written for $L = 1$ as

$$T(\vec{q}\,',\vec{q}\,) = (2L+1)\left(f(\sqrt{s})\,\hat{q}\,'\cdot\hat{q} - ig(\sqrt{s})\,(\hat{q}\,'\times\hat{q})\cdot\vec{\sigma}\right) \qquad (L=1)\ , \tag{12}$$

one defines the two amplitudes at tree level, $f_-^{\rm tree}$ ($L=1$, $J=1/2$) and $f_+^{\rm tree}$ ($L=1$, $J=3/2$), as

$$\begin{aligned} f_+^{\rm tree} &= f+g \\ f_-^{\rm tree} &= f-2g\ , \end{aligned} \tag{13}$$

with

$$\begin{aligned} f_{ij}(\sqrt{s}) &= \frac{1}{3}\left\{-C_{ij}\frac{1}{4f^2}\,a_i\,a_j\left(\frac{1}{b_i}+\frac{1}{b_j}\right)+\frac{D_i^\Lambda D_j^\Lambda\left(1+\frac{q_i^0}{M_i}\right)\left(1+\frac{q_j^0}{M_j}\right)}{\sqrt{s}-\tilde{M}_\Lambda}\right. \\ &\left.+\frac{D_i^\Sigma D_j^\Sigma\left(1+\frac{q_i^0}{M_i}\right)\left(1+\frac{q_j^0}{M_j}\right)}{\sqrt{s}-\tilde{M}_\Sigma}+\frac{2}{3}\frac{D_i^{\Sigma^*}D_j^{\Sigma^*}}{\sqrt{s}-\tilde{M}_\Sigma^*}\right\}q_iq_j \end{aligned} \tag{14}$$

$$\begin{aligned} g_{ij}(\sqrt{s}) &= \frac{1}{3}\left\{C_{ij}\frac{1}{4f^2}\,a_i\,a_j\left(\frac{1}{b_i}+\frac{1}{b_j}\right)-\frac{D_i^\Lambda D_j^\Lambda\left(1+\frac{q_i^0}{M_i}\right)\left(1+\frac{q_j^0}{M_j}\right)}{\sqrt{s}-\tilde{M}_\Lambda}\right. \\ &\left.-\frac{D_i^\Sigma D_j^\Sigma\left(1+\frac{q_i^0}{M_i}\right)\left(1+\frac{q_j^0}{M_j}\right)}{\sqrt{s}-\tilde{M}_\Sigma}+\frac{1}{3}\frac{D_i^{\Sigma^*}D_j^{\Sigma^*}}{\sqrt{s}-\tilde{M}_\Sigma^*}\right\}q_iq_j\ , \end{aligned} \tag{15}$$

where i,j are channel indices. Using Eq. (10), one obtains

$$\begin{aligned} f_+ &= [1-f_+^{\rm tree}G]^{-1}f_+^{\rm tree}\ , \\ f_- &= [1-f_-^{\rm tree}G]^{-1}f_-^{\rm tree}\ . \end{aligned} \tag{16}$$

These two equations are analogous to solving the Bethe-Salpeter equation. The Σ^* pole for $I=1$ is contained in the f_+ amplitude while the f_- amplitude includes the Λ and Σ poles for $I=0$ and $I=1$, respectively. As mentioned in Ref. [38], the unitarization procedure will shift the mass from a starting bare mass $\tilde{M}_\Lambda$, $\tilde{M}_\Sigma$, $\tilde{M}_{\Sigma^*}$ to the physically observed mass.

As one can see from these equations, the amplitudes $f_+^{\rm tree}$, $f_-^{\rm tree}$ in the diagonal meson-baryon channels contain the factor $\vec{q}^{\,2}$, with $\vec{q}$ the on-shell c.m. momentum of the meson in this channel. For transition matrix elements from channel i to j the corresponding factor is q_iq_j, where the energy and momentum of the meson in a certain channel are given by the expressions

$$E_i = \frac{s+m_i^2-M_i^2}{2\sqrt{s}}\ ;\quad q_i = \sqrt{E_i^2-m_i^2}\ , \tag{17}$$

which also provide the analytical extrapolation below the threshold of the channel, where q_i becomes purely imaginary.

III. IN-MEDIUM $\bar{K}N$ INTERACTION

The properties of the $\bar{K}$ in the nuclear medium are obtained by incorporating the corresponding medium modifications in the effective $\bar{K}N$ interaction.

A. Pauli blocking and self-energy effects

One of the sources of density dependence comes from the Pauli principle, which prevents the scattering to intermediate nucleon states below the Fermi momentum. This is implemented by replacing the free nucleon propagator in the loop function by the corresponding in-medium one.

Another source of density dependence is related to the fact that all mesons and baryons in the intermediate loops interact with the nucleons of the Fermi sea and their properties are modified with respect to those in free space.

The binding effects on the baryons are taken within a mean-field approach consisting in adding, to the single-particle energies, a momentum-independent potential. In the case of nucleons, we take $U = U_0\rho/\rho_0$, where $\rho_0 = 0.17$ fm^{-3} is normal nuclear matter density, and $U_0 = -70$ MeV , which is in agreement with numerous nuclear matter calculations with realistic interactions [43, 44]. On the other hand, we use the parametrization of Ref. [45] for Λ, $U^\Lambda = A\rho + B\rho^\gamma$ with $A = -340$ fm^{-3}, $B = 1087.5$ fm^6 and $\gamma = 2$. This parametrization shows a saturation behaviour and can be used in the study of densities beyond ρ_0. Finally, since the situation for the Σ-nucleus potential is unclear, we use for our calculations the attractive potential $U^\Sigma = -30\rho/\rho_0$ MeV, as commonly accepted for low densities [46, 47]. One of the outputs of the present study is the Λ and Σ self-energies in the medium, which we obtain by looking at the shift of their respective poles in the scattering matrix. A good degree of self-consistency is obtained between the input Λ and Σ potentials and their corresponding output, which agree within 10 % as will be seen in Sect. IV.

The nuclear medium effects on the mesons will be included through the corresponding self-energy. We will consider the dressing of the $\bar{K}$ and π mesons. The π self-energy can be found in Refs. [27, 48]. It consists of a small s-wave part plus a p-wave part, which is constructed by allowing the pion to couple to particle-hole, Δ-hole and two-particle-hole excitations modified by nuclear short-range correlations. The $\bar{K}$ self-energy is obtained from the s- and p-wave contributions to the in-medium $\bar{K}N$ amplitude as explicitly shown in Sect. III D.

From the meson self-energies, we can construct the dressed meson propagator ($i = \bar{K}$,π)

$$D_i(q^0, \vec{q}, \rho) = \frac{1}{(q^0)^2 - \vec{q}^{\,2} - m_i^2 - \Pi_i(q^0, \vec{q}, \rho)} \ , \tag{18}$$

and the corresponding spectral density

$$S_i(q^0, \vec{q}, \rho) = -\frac{1}{\pi}\mathrm{Im}\, D_i(q^0, \vec{q}, \rho) = -\frac{1}{\pi}\frac{\mathrm{Im}\Pi_i(q^0, \vec{q}, \rho)}{\mid (q^0)^2 - \vec{q}^{\,2} - m_i^2 - \Pi_i(q^0, \vec{q}, \rho) \mid^2} \ . \tag{19}$$

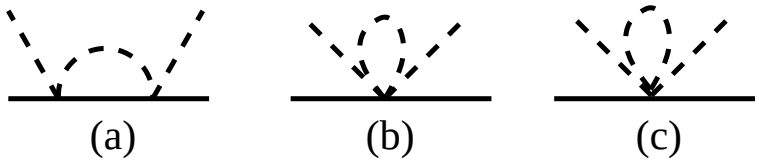

FIG. 1: On-shell (a), off-shell (b) and tadpole (c) contributions for the s-wave amplitude in free space.

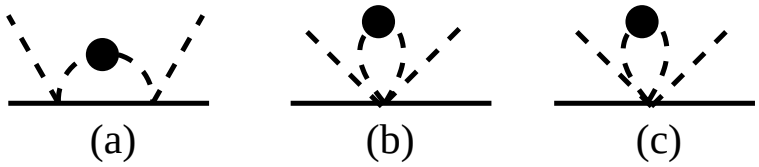

FIG. 2: On-shell (a), off-shell (b) and tadpole (c) contributions for the s-wave amplitude including self-energy insertions.

B. s-wave in-medium amplitudes

The calculation of the in-medium amplitudes requires a similar unitarization procedure as that performed in free space. A key simplification in evaluating the free space amplitudes was the factorization of the on-shell interaction kernel out of the loop function. In this section we will show that the on-shell factorization is still valid for the in-medium s-wave amplitudes.

We first recall the arguments given in Ref. [10] to justify the validity of the on-shell factorization in free space. Taking the structure of the s-wave kernel given in Eq. (4), the off-shell dependence of the loop function of Fig. 1(a) from the two vertices goes as

$$(k^0+q^0)^2 = (2\,k^0+q^0-k^0)^2 = (2\,k^0)^2 + 4\,k^0\,(q^0-k^0) + (q^0-k^0)^2\ . \tag{20}$$

The first term on the right-hand side of this equation accounts for the on-shell contribution in the vertices. The second and third terms cancel the intermediate baryon propagator in the loop in the heavy baryon approach ($p^0 \approx E(\vec{P}-\vec{q})$), which becomes $(k^0-q^0)^{-1}$, as can be seen from Eq. (11). The resulting off-shell contribution has the structure of Fig. 1(b), which will be conveniently canceled by a tadpole term, Fig. 1(c), in a suitable renormalization scheme.

In the nuclear medium, when we make self-energy attachments in the meson line, we find contributions as that shown in Fig. 2 and, given the structure of the off-shell part, Fig. 2(b), and the tadpole, Fig. 2(c), the cancellation that we had before still holds. This justifies the use of the on-shell vertices in the medium for the s-wave. Actually, the changes due to Pauli blocking in the nucleon line for the off-shell terms are shown to vanish below. Indeed,

the Pauli blocking correction to the loop integral of diagram 1(a) from the first off-shell contribution of Eq. (20) is:

$$\delta G_l^{\rm Pauli} \;=\; i\int \frac{d^4q}{(2\pi)^4}\,\frac{M_l}{E_l(\vec{P}-\vec{q})}\,(q^0-k^0)\,\frac{1}{q^2-m_l^2+i\epsilon}\,\times \\ \left\{\frac{1-n(\vec{P}-\vec{q})}{P^0-q^0-E_l(\vec{P}-\vec{q})+i\epsilon}+\frac{n(\vec{P}-\vec{q})}{P^0-q^0-E_l(\vec{P}-\vec{q})-i\epsilon}\right. \\ \left.-\frac{1}{P^0-q^0-E_l(\vec{P}-\vec{q})+i\epsilon}\right\}\,, \tag{21}$$

with $P^0=k^0+p^0$. Since the Pauli blocking corrections are only operative at the nucleon pole, one finds

$$\delta G_l^{\rm Pauli} \;=\; i\int \frac{d^4q}{(2\pi)^4}\,\frac{M_l}{E_l(\vec{P}-\vec{q})}\,(q^0-k^0)\,\frac{1}{q^2-m_l^2+i\epsilon}\,\times \\ 2\,i\,\pi\,n(\vec{P}-\vec{q})\,\delta(p^0+k^0-q^0-E_l(\vec{P}-\vec{q}))\;. \tag{22}$$

Since $p^0-E_l(\vec{P}-\vec{q})\approx 0$ in the heavy-baryon approach, the delta function forces the factor (q^0-k^0) to be zero and the correction $\delta G_l^{\rm Pauli}$ vanishes. An identical argument holds for the other off-shell term, which is proportional to $(q^0-k^0)^2$.

Generalizing these findings to all orders, it is concluded that the on-shell factorization can be applied for the in-medium s-wave amplitudes and the loop function is simply the integral of a meson and a baryon propagator, conveniently modified by self-energy insertions and binding corrections, namely:

$$G^s_{\bar{K}N}(P^0,\vec{P},\rho)=\int_{|\vec{q}|<q^{\rm lab}_{\rm max}}\frac{d^3q}{(2\pi)^3}\,\frac{M_N}{E_N(\vec{P}-\vec{q})}\,\times \\ \left[\int_0^\infty d\omega S_{\bar{K}}(\omega,\vec{q},\rho)\frac{1-n(\vec{P}-\vec{q})}{P^0-\omega-E_N(\vec{P}-\vec{q})+i\epsilon}\right. \\ \left.+\int_0^\infty d\omega S_K(\omega,\vec{q},\rho)\frac{n(\vec{P}-\vec{q})}{P^0+\omega-E_N(\vec{P}-\vec{q})+i\epsilon}\right]\,, \tag{23}$$

for $\bar{K}N$ states and

$$G^s_{\pi Y}(P^0,\vec{P},\rho) \;=\; \int_{|\vec{q}|<q^{\rm lab}_{\rm max}}\frac{d^3q}{(2\pi)^3}\,\frac{M_Y}{E_Y(\vec{P}-\vec{q})}\int_0^\infty d\omega S_\pi(\omega,\vec{q},\rho) \\ \times\;\frac{1}{P^0-\omega-E_Y(\vec{P}-\vec{q})+i\epsilon}\,, \tag{24}$$

for $\pi\Lambda$ or $\pi\Sigma$ states, where $P=(P^0,\vec{P}\,)$ is the total four-momentum and $\vec{q}$ is the meson momentum in the laboratory system.

For $\eta\Lambda$, $\eta\Sigma$ and $K\Xi$ states, no self-energy insertions are incorporated in the meson lines and we can use the loop integral in free space of Eq. (11), modified by including the binding potential in the baryon energy.

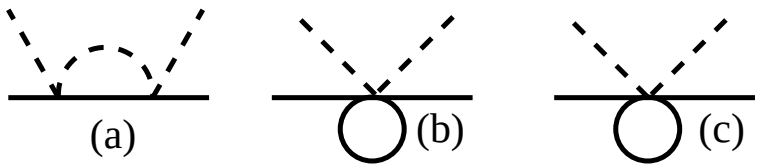

FIG. 3: On-shell (a), off-shell (b) and tadpole (c) contributions for the p-wave amplitude in free space.

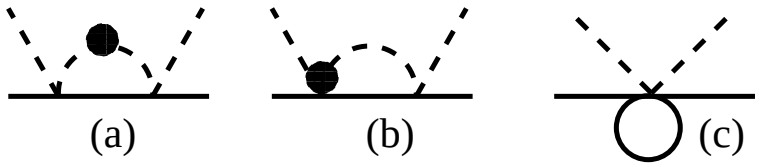

FIG. 4: On-shell (a), off-shell (b) and tadpole (c) contributions for the p-wave amplitude including self-energy insertions.

The in-medium s-wave amplitudes are then obtained by solving the coupled-channel Eq. (10) with these medium modified loop functions.

C. p-wave in-medium amplitudes

The situation is different for the p-wave amplitudes. The $\vec{q}^{\,2}$ dependence from the vertices in the one-loop contribution to the p-wave amplitude can be separated into an on-shell part, $\vec{q}^{\,2}_{\rm on}$, and an off-shell part, $\vec{q}^{\,2} - \vec{q}^{\,2}_{\rm on}$. In free space, the one-loop contribution, splitted into its on-shell and off-shell parts, is represented by the diagrams of Fig. 3(a) and (b), respectively. The factor $\vec{q}^{\,2} - \vec{q}^{\,2}_{\rm on}$ can be shown to cancel the meson propagator (see Ref. [41]) and, hence, the off-shell contribution, Fig. 3(b), is canceled by the tadpole term of Fig. 3(c).

In the medium, when the meson propagator is dressed, one encounters the situation of Fig. 4, where in the diagram 4(b) it is seen that the factor $\vec{q}^{\,2} - \vec{q}^{\,2}_{\rm on}$ only cancels one of the two intermediate meson propagators and, furthermore, there are no medium corrections for the self-energy insertion in the inexistent intermediate mesons of the tadpole term in Fig. 4(c). Hence, in the medium, we do not find the cancellation between the off-shell part and the tadpole term that applied to the s-wave amplitudes. However, there is no problem if we add, to the free loop function (for which the on-shell prescription is valid) the medium corrections calculated using the full off-shell $\vec{q}^{\,2}$ contribution of the vertices, according to the following replacement

$$G_l^p(s) \to G_l^p(s) + \frac{1}{\vec{q}^{\,2}_{on}}[I_{\rm med}(s) - I_{\rm free}(s)] \ , \tag{25}$$

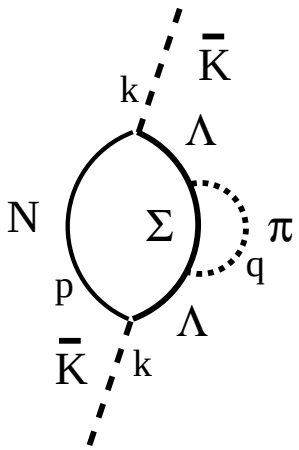

FIG. 5: p-wave contribution to the $\bar{K}$ self-energy

where

$$
\begin{aligned}
I_{\rm med}(s) &= i\int \frac{d^4q}{(2\pi)^4}\vec{q}^{\,2} D_M(q) G_B(P-q) \\
I_{\rm free}(s) &= i\int \frac{d^4q}{(2\pi)^4}\vec{q}^{\,2} D^0_M(q) G^0_B(P-q)\ ,
\end{aligned}
\tag{26}
$$

where G^p_l is the free loop of Eq. (11), $D_M(q)$ and $G_B(P-q)$ stand for the meson and baryon propagator in the medium, respectively, while $D^0_M(q)$ and $G^0_B(P-q)$ correspond to those in free space. The tadpole terms have been assumed to cancel in the difference on the r.h.s. of Eq. (25).

In order to see explicitly the problems of the on-shell factorization, let us evaluate the contribution to the antikaon self-energy shown in Fig. 5, where the $\bar{K}$ couples to a ΛN^{-1} excitation and the Λ line contains a $\Sigma\pi$ self-energy insertion. The corresponding expression for the self-energy is

$$
\begin{aligned}
-i\,\Pi(k) \;=\; & g^2_{N\Lambda K}\int \frac{d^4p}{(2\pi)^4}(-2\vec{k}^{\,2})\frac{in(\vec{p})}{p^0-E(\vec{p})+i\varepsilon}\left(\frac{i}{p^0+k^0-E_\Lambda(\vec{p}+\vec{k}\,)+i\varepsilon}\right)^2 \\
& \times g^2_{\Lambda\Sigma\pi}\int \frac{d^4q}{(2\pi)^4}(-\vec{q}^{\,2})\frac{i}{p^0+k^0-q^0-E_\Sigma(\vec{p}+\vec{k}-\vec{q}\,)}\,\frac{i}{q^{0\,2}-\vec{q}^{\,2}-m^2_\pi+i\varepsilon}\ .
\end{aligned}
\tag{27}
$$

Applying Cutkosky rules

$$
\begin{aligned}
\Pi(k) &\to 2\,i\,{\rm Im}\Pi(k) \\
G_N(p) &\to 2\,i\,\theta(p^0)\,{\rm Im}G_N(p) \\
G_\Sigma(p+k-q) &\to 2\,i\,\theta(p^0+k^0-q^0){\rm Im}G_\Sigma(p+k-q) \\
D_\pi(q) &\to 2\,i\,\theta(q^0)\,{\rm Im}D_\pi(q)
\end{aligned}
\tag{28}
$$

to evaluate the imaginary part corresponding to a cut producing $\Sigma\pi N^{-1}$ states, we obtain

$$\begin{aligned}\mathrm{Im}\Pi(k) \;=\; & -g^2_{N\Lambda K} g^2_{\Lambda\Sigma\pi} \vec{k}^{\,2} \int \frac{d^3p}{(2\pi)^3} n(\vec{p}\,) \left(\frac{1}{p^0 + k^0 - E_\Lambda(\vec{p}+\vec{k}\,)} \right)^2 \\ & \times \int \frac{d^3q}{(2\pi)^3} \frac{\vec{q}^{\,2}}{2\omega(\vec{q}\,)} \delta(k^0 + E_N(p) - \omega(\vec{q}\,) - E_\Sigma(\vec{p}+\vec{k}-\vec{q}\,)) \; . \end{aligned} \tag{29}$$

If one blindly applies the on-shell factorization to this p-wave contribution, the factor $\vec{q}^{\,2}$ would be replaced by $\vec{q}^{\,2}_{\rm on}$ and taken out of the integral over the running variable $\vec{q}$. For an incident antikaon energy, k^0, such that $m_\pi + M_\Sigma < k^0 + M_N$ we would find $\vec{q}^{\,2}_{\rm on} > 0$. If this value of the kaon energy is below the kaon mass, namely $k^0 + M_N < m_K + M_N$, then the corresponding on-shell antikaon momentum would fulfill $\vec{k}^{\,2} < 0$ and, in this case, we would end up having a positive contribution to the imaginary part of the $\bar{K}$ self-energy, hence violating the principle of causality. However, this would not be a real problem since, in the medium, one needs to keep the proper independence of the kaon energy-momentum variables, and this amplitude will be corrected, as explained at the end of this section, by a factor $k^2_{\rm lab}/k^2$, where $\vec{k}_{\rm lab}$ is the antikaon momentum in the laboratory system, which is a well defined real quantity. Having this correction in mind, the pathology would then occur when $k^0 + M_N < m_\pi + M_\Sigma$, since in this case $\vec{q}^{\,2}_{\rm on} < 0$, hence leaving a positive contribution to the imaginary part of the $\bar{K}$ self-energy for a kaon with momentum $\vec{k}_{\rm lab}$ and energy $k^0 < m_\pi + M_\Sigma - M_N$.

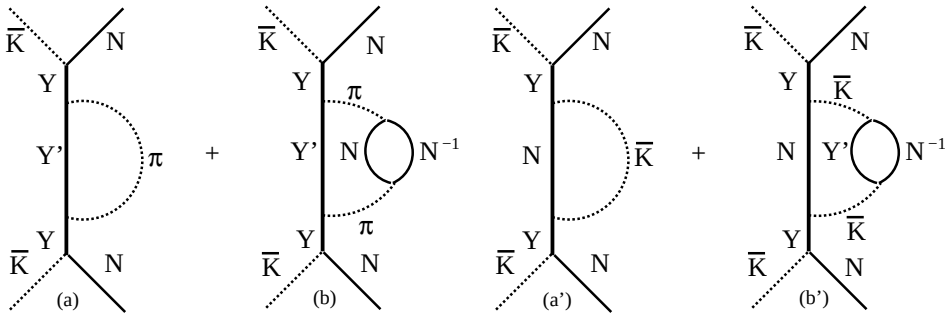

FIG. 6: Diagrams contributing to the $\bar{K}N$ p-wave amplitude including intermediate pions (a,b) and intermediate kaons (a',b')

Another ingredient that has to be considered when dealing with p-wave amplitudes in the medium is the effect of nuclear short-range correlations. Diagrams such as that of Fig. 6 are present in the in-medium p-wave $\bar{K}N$ amplitude and, therefore, the π ($\bar{K}$) propagators connecting a bubble to a baryonic line (see Figs. 6(b) and (b')) or to another bubble should be modified in order to account for the fact that the nucleon-nucleon (hyperon-nucleon) interaction is not only driven by one-pion (one-kaon) exchange.

Let's take the case of pions explicitly. The contribution of the diagram of Fig. 6(b) reads

$$F^4(\vec{q}\,)\vec{q}D^0(q^0,\vec{q}\,) \left(\frac{f_{\pi NN}}{m_\pi} \right)^2 U(q^0,\vec{q}\,)\vec{q}^{\,2} D^0(q^0,\vec{q}\,)\vec{q}$$

$$= F^4(\vec{q})\delta_{il}q_i D^0(q^0,\vec{q})\left(\frac{f_{\pi NN}}{m_\pi}\right)^2 U(q^0,\vec{q})q_j q_j D^0(q^0,\vec{q})q_l, \tag{30}$$

where $U(q^0,\vec{q})$ corresponds to the Lindhard function and $F(\vec{q}) = \Lambda^2/(\Lambda^2+\vec{q}^{\,2})$ with $\Lambda = 1$ GeV. The effect of short-range correlations is incorporated by replacing the exchanged pion in Fig. 6(b) by a fully correlated interaction, which is achieved by the following replacement in Eq. (30)

$$F^2(\vec{q})^2 q_i q_j D^0(q^0,\vec{q}) \to V_l \hat{q}_i\hat{q}_j + V_t(\delta_{ij}-\hat{q}_i\hat{q}_j)\ , \tag{31}$$

where

$$V_l \ = \ (\vec{q}^{\,2}D^0(q^0,\vec{q}) + g')F^2(\vec{q}), \quad V_t = g'F^2(\vec{q})\ ,$$

with $g' \simeq 0.6$ being the usual Landau-Migdal parameter [49]. Then Eq. (30) reads

$$\begin{aligned}
&\delta_{il}\left[V_l\hat{q}_i\hat{q}_j + V_t(\delta_{ij}-\hat{q}_i\hat{q}_j)\right]\left(\frac{f_{\pi NN}}{m_\pi}\right)^2 U(q^0,\vec{q})\left[V_l\hat{q}_j\hat{q}_l + V_t(\delta_{jl}-\hat{q}_j\hat{q}_l)\right] \\
&= \delta_{il}\left[V_l^2\hat{q}_i\hat{q}_l + V_t^2(\delta_{il}-\hat{q}_i\hat{q}_l)\right]\left(\frac{f_{\pi NN}}{m_\pi}\right)^2 U(q^0,\vec{q})\ .
\end{aligned} \tag{32}$$

Since the longitudinal and transverse components are decoupled from each other, successive iterations lead to

$$\frac{V_l^2\left(\frac{f_{\pi NN}}{m_\pi}\right)^2 U(q^0,\vec{q})}{1-V_l\left(\frac{f_{\pi NN}}{m_\pi}\right)^2 U(q^0,\vec{q})} + 2\frac{V_t^2\left(\frac{f_{\pi NN}}{m_\pi}\right)^2 U(q^0,\vec{q})}{1-V_t\left(\frac{f_{\pi NN}}{m_\pi}\right)^2 U(q^0,\vec{q})}\ . \tag{33}$$

Using the fact that the Lindhard function and p-wave self-energy are related by $(f_{\pi NN}/m_\pi)^2\, U(q^0,\vec{q}) = \Pi^p(q^0,\vec{q})/(\vec{q}^{\,2}F^2(\vec{q}))$ and summing the contribution of the first diagram, Fig. 6(a), the full dressed pion propagator without correlations $D(q^0,\vec{q})$ has to be substituted by

$$\begin{aligned}
&F^2(\vec{q})\vec{q}^{\,2}D(q^0,\vec{q}) \to F^2(\vec{q})\vec{q}^{\,2}\frac{1}{q^{0\,2}-\vec{q}^{\,2}-m_\pi^2-\Pi_\pi^s} + \\
&\frac{V_l^2\Pi^p(q^0,\vec{q})/(\vec{q}^{\,2}F^2(\vec{q}))}{1-V_l\Pi^p(q^0,\vec{q})/(\vec{q}^{\,2}F^2(\vec{q}))} + 2\frac{V_t^2\Pi^p(q^0,\vec{q})/(\vec{q}^{\,2}F^2(\vec{q}))}{1-V_t\Pi^p(q^0,\vec{q})/(\vec{q}^{\,2}F^2(\vec{q}))}\ ,
\end{aligned} \tag{34}$$

where the s-wave piece of the self-energy has been included in the definition of the free pion propagator. Alternatively,

$$\begin{aligned}
&F^2(\vec{q})\vec{q}^{\,2}D(q^0,\vec{q}) \to \\
&\frac{1-g'F^2(\vec{q})V_l^{-1}+g'\Pi^p(q^0,\vec{q})/\vec{q}^{\,2}}{V_l^{-1}-\Pi^p/(\vec{q}^{\,2}F^2(\vec{q}))} + 2\frac{V_t^2\Pi^p(q^0,\vec{q})/(\vec{q}^{\,2}F^2(\vec{q})}{1-V_t\Pi^p(q^0,\vec{q})/(\vec{q}^{\,2}F^2(\vec{q}))}\ .
\end{aligned} \tag{35}$$

A similar expression is obtained for the antikaon propagator when the diagram of Fig. 6(b') and its subsequent iterations, all corrected by the short-range effects of the hyperon-nucleon interaction, are added to the diagram of Fig. 6(a').

The in-medium p-wave amplitudes are finally obtained by solving the same equations as in free space, Eqs. (16), taking the tree amplitudes from Eqs. (13)-(15), evaluated with on-shell momentum values depending on $\sqrt{s}$, and using the in-medium meson-baryon propagator of Eq. (25), which incorporates the proper $\vec{q}^{\,2}$ dependence in the medium corrections to the p-wave amplitudes, as well as Pauli blocking effects, dressing of the mesons, binding potentials for the baryons and nuclear short-range correlations.

Finally, the amplitudes need to be corrected to incorporate, in the external states, the proper off-shell momentum, which we write for convenience in terms of the laboratory variables. Furthermore, in going from c.m. to lab momenta, the vertex recoil factors also need to be corrected. Technically this is implemented by the following expression:

$$
\begin{aligned}
(f_+)^{\rm med}_{ij} &= ([1-f_+^{\rm tree}G]^{-1}f_+^{\rm tree})_{ij}\frac{(q_{\rm lab})_i(q_{\rm lab})_j}{(q_{\rm on})_i(q_{\rm on})_j}\left(1-\frac{(q^0_{\rm lab})_i}{M_{\Sigma^*}}\right)\left(1-\frac{(q^0_{\rm lab)_j}}{M_{\Sigma^*}}\right)\\
(f_-)^{\rm med}_{ij} &= ([1-f_-^{\rm tree}G]^{-1}f_-^{\rm tree})_{ij}\frac{(q_{\rm lab})_i(q_{\rm lab})_j}{(q_{\rm on})_i(q_{\rm on})_j}\frac{\left(1-\frac{(q^0_{\rm lab})_i}{2\overline{M}}\right)\left(1-\frac{(q^0_{\rm lab})_j}{2\overline{M}}\right)}{\left(1+\frac{(q^0_{\rm on})_i}{2M}\right)\left(1+\frac{(q^0_{\rm on})_j}{2M}\right)}\ ,
\end{aligned}
\tag{36}
$$

where $q_{\rm on}$ and $q_{\rm lab}$ stand, respectively, for the on-shell momentum and the momentum in the laboratory system, M is the nucleon mass and $\overline{M}$ is the average Σ-Λ mass. Actually, for the f_- amplitude we could separate between the $I=0$ and $I=1$ amplitudes and introduce the recoil corrections with the corresponding Λ and Σ masses, respectively. However, given the similar masses of the Σ and Λ, the use of an averaged mass induces errors of less than 1%. We note that, by correcting the external meson-baryon channels with the relativistic recoil factors appropriate for pole-type terms, we are also performing an unnecessary correction on the contact term of the p-wave amplitudes, the first term in Eqs. (14),(15). However, this induced error is negligible since this term is very small compared to the Λ, Σ and Σ^* pole contributions to the p-wave amplitude.

D. $\bar{K}$ self-energy

The $\bar{K}$ self-energy in dense nuclear matter is obtained by summing the in-medium $\bar{K}$ interaction $T_{\bar{K}N}$ for s- and p- waves over the Fermi sea of nucleons according to

$$
\Pi_{\bar{K}}(q^0,\vec{q},\rho) = 4\int\frac{d^3p}{(2\pi)^3}\,n(\vec{p})\,T_{\bar{K}N}(P^0,\vec{P},\rho)\ , \tag{37}
$$

where $P^0=q^0+E(p)$ and $\vec{P}=\vec{q}+\vec{p}$ are the total energy and momentum in the lab frame and the values (q^0,$\vec{q}$) stand for the energy and momentum of the $\bar{K}$ in this frame. Note that the $\bar{K}$ self-energy must be determined self-consistently, since it is obtained from the in-medium interaction which uses $\bar{K}$ propagators which themselves include the self-energy being calculated.

We finally remark that the recoil corrections discussed at the end of the previous section assumed the nucleons to be at rest in the laboratory frame. However, in the evaluation

of the $\bar{K}$ self-energy, one works in a frame where the nuclear Fermi sea is at rest and the recoil corrections will then have to take into account the Fermi motion of nucleons. These corrections, which induce a small contribution to the s-wave amplitudes, are studied in detailed in Ref. [50] and are incorporated in our calculations. For completeness, we reproduce here the expression for these p-wave induced Fermi motion corrections to the s-wave self-energy:

$$\Pi_{\bar{K}}^{(s,\mathrm{ind})}(q^0,\vec{q},\rho) = \frac{3}{5}k_F^2(q^0)^2\left[\frac{1}{4}\left(\frac{1}{M_N}+\frac{1}{M_\Lambda}\right)^2 D_{\bar{K}N\Lambda}^2 U_\Lambda(q^0,\vec{q}) + \frac{1}{4}\left(\frac{1}{M_N}+\frac{1}{M_\Sigma}\right)^2 D_{\bar{K}N\Sigma}^2 U_\Sigma(q^0,\vec{q}) + \left(\frac{1}{M_{\Sigma^*}}\right)^2 D_{\bar{K}N\Sigma^*}^2 U_{\Sigma^*}(q^0,\vec{q})\right] \quad (38)$$

where U_Y stands for the hyperon-hole Lindhard function and $D_{\bar{K}NY}$ is the coupling constant of the $\bar{K}NY$ vertex.

IV. RESULTS

In Fig. 7 we present our results for the $I=0$ J^P=1/2$^+$ resonances, the s-wave $\Lambda(1405)$ (right panel) and the p-wave $\Lambda(1115)$ (left panel). We show the imaginary part of the $\bar{K}N \to \bar{K}N$ amplitude as a function of $\sqrt{s}$ for two values of the momentum P. The p-wave amplitude is divided by the square of the $\bar{K}N$ on-shell momentum corresponding to each value of $\sqrt{s}$. The free space amplitudes (dotted lines) are compared with the in-medium ones at $\rho=\rho_0=0.17$ fm^{-3} for two approximations: dressing the antikaons self-consistently (dashed lines) and considering also the in-medium effects on the properties of the pions (solid lines). The apparent width of the $P=0$ $\Lambda(1115)$ is fictitious and comes from a small width inserted in the Λ and Σ pole driving terms to facilitate the convergence of the self-consistent calculations. At finite total momentum the width is physical since the Λ can excite, via its interactions with nucleons in the Fermi sea, intermediate $\Lambda N N^{-1}$ states having the same total momentum P. We find, similarly to what is found in the model of Ref. [37], that the $\Lambda(1115)$ acquires an attractive shift of about 10 MeV when the self-consistent dressing of the antikaons is considered. If the in-medium pion self-energy is also incorporated, the $\Lambda(1115)$ develops an attraction three times larger, of 28 MeV, in accordance to what is demanded by hypernuclear spectroscopic data [51] and also to what is obtained from nuclear matter microscopic calculations using the recent meson-exchange YN potentials [52–55]. The reason lies in that the dressing of the pions implicitly incorporates, through the coupling of the pion to ph states, an important piece of the ΛN interaction, namely the $\Lambda N \to \Sigma N$ transition potential mediated by pion-exchange.

The $\Lambda(1405)$ shows the features that were already observed in our earlier paper [27] and which we summarize here. Since the self-consistent dressing lowers the antikaon mass by about 50 MeV and, in addition, a stronger binding potential is taken for nucleons than for hyperons, the $\bar{K}N$ threshold gets effectively lowered in the medium and the $\Lambda(1405)$ is

dynamically generated at a lower value of $\sqrt{s}$ (dashed line). When pions are dressed new channels are available, such as ΛNN^{-1} or ΣNN^{-1}, so the $\Lambda(1405)$ gets strongly diluted and the peak appears very close to the free space position. We note the cusp effect that appears at an energy corresponding to the in-medium $\pi\Sigma$ threshold as a consequence of the opening of this channel on top of the already opened ΛNN^{-1} and ΣNN^{-1} ones.

The $I = 1$ resonances are shown in Fig. 8. The left panels display the imaginary part of the $\bar{K}N \to \bar{K}N$ amplitude divided by the square of the $\bar{K}N$ on-shell momentum in the $J = 1/2^+$ p-wave corresponding to the $\Sigma(1195)$, while the right panels show the imaginary part of the $\pi\Lambda \to \pi\Lambda$ amplitude divided by the square of the $\pi\Lambda$ on-shell momentum in the $J = 3/2^+$ p-wave corresponding to the $\Sigma(1385)$. The width of the $\Sigma(1195)$ is a reflection of the decay channel $\Sigma N \to \Lambda N$, which is incorporated as soon as the antikaon or/and the pions are dressed. However, we expect pion dressing to play a stronger role due to the larger value of the coupling constants involved and to the relative size between the pion and kaon propagators. We indeed observe that pion dressing produces an additional attraction of about 35 MeV to that obtained with the approximation of dressing only the antikaons, which only produces an attraction of 2 MeV. This last value is in contrast with the 10 MeV attraction found in Ref. [37].

The $\Sigma(1385)$ moves very little in the medium, around 7 MeV from its free space position, for both approximations. Again, in the approximation that only dresses the antikaons this moderate effect differs from the 60 MeV attraction quoted in Ref. [37]. The 30 MeV width of the $\Sigma(1385)$ in free space increases by about 10 MeV when antikaons are dressed, due to the opening of new decay channels such as $\Sigma^* N \to \Lambda N,\ \Sigma N$ through the coupling of the $\bar{K}$ to YN^{-1} excitations. For similar reasons mentioned above in the case of the $\Sigma(1195)$, the decay width into these new decay channels increases spectacularly when the pions are also dressed, giving rise to a Σ^* in the medium having a width of around 80 MeV, consistently to what is found in Ref. [56], where the self-energy of the $\Sigma(1385)$ is evaluated explicitly. Here, instead, we make a complete unitary theory of the p-wave $\bar{K}N$ scattering in the medium, where all particles and resonances are renormalized automatically at the same time.

As one can see from Fig. 8 we obtain an attractive Σ self-energy in the medium of around 35 MeV at $\rho{=}\rho_0$, much in line with what one obtains from [46] and [57]. In the literature one finds potentials coming from fits to data of Σ-atoms with a chosen parametrization that leads to repulsion at short distances [58], while they are attractive at large distances. A similar behaviour is obtained in models using Dirac phenomenology [59]. Other theoretical studies using chiral perturbation theory find a net repulsion at long distances of the order of 59 MeV at nuclear matter density [60]. The situation is thus confusing and the only experimental evidence is that atoms require an attraction at the relatively large distances probed.

There is another type of experimental information provided by the study of the Σ-production spectrum in the (π^-, K^+) reactions. Analysis of the spectra within the distorted wave approximation for the pion and kaon waves leads to a repulsive Σ-nucleus potential [61–63]. Yet, here we must make some comment to clarify the origin of these results. The

analyses of [61–63] use distorted waves for the pions and kaons or make use of the efficient and equivalent Green's function method [64]. This is appropriate when one studies coherent production or elastic scattering, but not for inclusive reactions as is the case there. The reason is simple: the optical potentials used for pions and kaons have an imaginary part that comes from quasi-elastic collisions and absorption. This separation is done in potentials like the one given in [65] for pions or in [40] for kaons. In the use of the distorted waves the imaginary part of the potential depletes the strength of the waves, in other words, every time there is a quasi-elastic collision or absorption of the K or π the event is removed. This is correct when one looks at the formation of the ground state since any quasi-elastic collision excites the nucleus. However, in inclusive reactions where one sums over all final nuclear states, this is not correct because if there is a quasi-elastic collision the particle is still there and can be detected, while the calculation has removed it. It is then clear that the calculation will push to get a repulsive Σ-nucleus potential to prevent the Σ from being too close to the nucleus where the inappropriate calculation of the distorted pion and kaon waves would remove too many events. The experimental situation is thus confusing and the only firm information is the attractive potential felt by the Σ^- at the small densities probed by the atoms.

The self-energy of the antikaon at $\rho = 0.17$ fm^{-3} as a function of the antikaon energy is displayed in Fig. 9 for two values of the antikaon momentum, $q = 0$ and 450 MeV/c. We show the s-wave component of the self-energy for the approximation that only dresses antikaons self-consistently (dotted line) and when the dressing of pions is also incorporated (dashed lines). These results correspond to those obtained in Ref. [27]. The small amount of imaginary part at subthreshold antikaon energies and zero momentum is due to s-wave excitations of the type $\bar{K}NN \to \Sigma N,\ \Lambda N$, where the nucleons have assumed to feel a potential of -70 MeV and the hyperons one of -30 MeV. Note that some extra enhancement of the imaginary part would be visible in that region if we used a more moderate attraction for the nucleon potential. The solid line shows the results when the new p-wave components calculated in the present work are also incorporated. In the case of zero antikaon momentum, the additional p-wave strength corresponds to the p-wave induced s-wave corrections described in Sect. III D (see also Ref. [50]), which produce a slight repulsion in the real part of the self-energy at the antikaon mass since the energies that come into play are above Λ, Σ and Σ^* excitation. The role of the p-wave self-energy is more evident for an antikaon momentum of 450 MeV/c. The imaginary part of the corresponding self-energy clearly displays the signals of ΣN^{-1} and $\Sigma^* N^{-1}$ components around 300 MeV and 550 MeV, respectively. More specifically, around 200 MeV below the antikaon mass, the width, $-2\mathrm{Im}\Pi_{\bar{K}}/(2q^0)$, increases considerably to about 160 MeV. At the same energy but for a more moderate momentum of 200 MeV/c, this quantity would be divided by a factor $(450/200)^2 \simeq 5$. Should the antikaon mode achieve such an amount of attraction, these results show that the width of the bound state would be appreciable due to the p-wave components of the $\bar{K}$ self-energy.

We next comment our results on the antikaon spectral function for the approximation that only dresses the antikaons in Fig. 10 and when pions are also dressed in Fig. 11, for

three different densities, ρ=0.5ρ_0, ρ_0 and 2ρ_0. As it is evident from these plots, the antikaon spectral function is far from having a Breit-Wigner type of behavior. At zero momentum, one observes the antikaon quasiparticle peak, located at a lower energy than the position of the free antikaon pole, superimposed to a shoulder of slow fall off on the right-hand side, which corresponds to $\Lambda(1405)N^{-1}$ excitation. At normal nuclear matter density, the quasiparticle peak at zero momentum is displaced by about -60 MeV with respect to the free space position, while at a momentum of 450 MeV/c the displacement only amounts to about -5 MeV. We observe that, even at zero momentum, there is a change in the s-wave spectral function (dashed lines) when the p-wave strength is also included (solid lines), which is due to the p-wave induced s-wave Fermi motion corrections. As density increases, the quasiparticle peak at zero momentum gains attraction while the spectral function at an antikaon momentum of 450 MeV/c gets strongly diluted, especially when p-waves are incorporated. The small peak in Fig. 10 to the right of the main quasiparticle peak for the $q = 0$ spectral function at $2\rho_0$ is due to the p-wave induced s-wave component associated to $\Sigma^* N^{-1}$ excitations, which are located close to the dressed antikaon quasiparticle peak. When pions are also dressed the antikaon spectral functions displayed in Fig. 11 show similar features, although somewhat wider and more diluted.

We finally present in Fig. 12 results for the antikaon optical potential calculated as $\Pi_k(q, \varepsilon(q))/(2\varepsilon(q))$, where $\varepsilon(q)$ is the quasiparticle energy fulfilling $\varepsilon(q)^2 = m_K^2 + q^2 + \mathrm{Re}\Pi(q, \varepsilon(q))$, for three different densities ρ=0.5ρ_0, ρ_0 and 2ρ_0. The real and imaginary parts of the antikaon optical potential as functions of q are shown on the left panels, for the approximation that only dresses the antikaons, and on the right panels, when pions are also dressed. As density increases, the real part of the optical potential becomes more attractive. In the approximation that only dresses the antikaons self-consistently, the value of the optical potential at zero momentum goes from around -40 MeV at $\rho_0/2$ to -70 MeV at 2ρ_0. The width of this zero momentum state, which is twice the size of the corresponding imaginary part of the optical potential, decreases with density due to the loss of decaying phase-space as the antikaon gains attraction. This picture gets somewhat distorted when pions are also dressed. Whereas, in this case, the real part of the optical potential at zero momentum goes from about -30 MeV at $\rho_0/2$ to almost -80 MeV for 2ρ_0, the size of the imaginary part first increases (from $\rho_0/2$ until ρ_0) and then decreases fast (from ρ_0 to 2ρ_0). This is because part of the loss of decaying phase space with increasing density is compensated by the appearance of new decaying states, YNN^{-1}, the amount of which increases with increasing density. Our results are qualitatively very similar to those shown in Ref. [36], where a self-consistent calculation of the antikaon optical potential using the meson-exchange Jülich $\bar{K}N$ interaction was presented.

V. CONCLUSIONS

We have investigated the properties of the $\bar{K}$ self-energy in nuclear matter after incorporating the medium modifications on the s-wave and p-wave $\bar{K}N$ amplitudes, within the

context of a chiral unitary approach. The s-wave interaction is taken from the Weinberg-Tomozawa term and the p-wave collects a small contribution from this source and a large contribution from the Λ, Σ and $\Sigma(1385)$ pole terms. To account for the medium renormalization of the amplitudes, we include, in a self-consistent way, Pauli blocking effects, meson self-energies corrected by nuclear short-range correlations and baryon binding potentials.

We have payed a special attention to the modification of the p-waves, showing that for the in-medium corrections it is not possible to apply the on-shell factorization of the amplitudes, which is the standard procedure in free space.

The Λ and Σ in nuclear matter at saturation density feel an attractive potential of around -30 MeV, while the Σ^* stays pretty much at its free space position but its width is sensibly increased to about 80 MeV.

The $\bar{K}$ self-energy is evaluated as a function of laboratory energy q^0 and momentum $\vec{q}$, which are independent variables in the medium. The p-wave contributions to the antikaon self-energy are small for low momentum kaons. However, at large momentum values of about 450 MeV/c, one finds considerable strength at subthreshold energies coming from $\bar{K}N \to \Sigma$ conversion.

The $\bar{K}$ spectral function shows a distinct quasiparticle peak around 60 MeV below the antikaon mass from zero momentum. The peak moves to higher energy and gets closer to the free space position as the $\bar{K}$ picks up momentum. Thus, the consideration of p-waves does not help in increasing the binding energy of the $\bar{K}$ mode. The increased amount of strength at low antikaon energies of around 300 MeV when p-waves are included implies that, if the kaon mode was able to generate such an amount of attraction, the bound state would have an appreciable width. However, the antikaon optical potential obtained in the present work can only give $\bar{K}$ states in matter bound by no more than 50 MeV and having a width of the order of 100 MeV, in qualitative agreement with all existing self-consistent calculations.

Acknowledgments

L.T. wishes to acknowledge support from Gesellschaft für Schwerionenforschung and Alexander von Humboldt Foundation. This work is partly supported by contracts BFM2003-00856 and FIS2005-03142 from MEC (Spain) and FEDER, the Generalitat de Catalunya contract 2005SGR-00343, and the E.U. EURIDICE network contract HPRN-CT-2002-00311. This research is part of the EU Integrated Infrastructure Initiative Hadron Physics Project under contract number RII3-CT-2004-506078.

---

[1] J. A. Oller, E. Oset and A. Ramos, Prog. Part. Nucl. Phys. **45**, 157 (2000).

[2] R.H. Dalitz and S.F. Tuan, Ann. Phys. (N.Y.) **10**, 307 (1960).

[3] B. K. Jennings, Phys. Lett. B **176**, 229 (1986).

[4] J. Gasser and H. Leutwyler, Nucl. Phys. B **250**, 465 (1985).

[5] U. G. Meissner, Rept. Prog. Phys. **56**, 903 (1993).

[6] V. Bernard, N. Kaiser and U. G. Meissner, Int. J. Mod. Phys. E **4**, 193 (1995).

[7] A. Pich, Rept. Prog. Phys. **58**, 563 (1995).

[8] G. Ecker, Prog. Part. Nucl. Phys. **35**, 1 (1995).

[9] N. Kaiser, T. Waas and W. Weise, Nucl. Phys. A **612**, 297 (1997).

[10] E. Oset and A. Ramos, Nucl. Phys. A **635**, 99 (1998).

[11] J. A. Oller and U. G. Meissner, Phys. Lett. B **500**, 263 (2001).

[12] M. F. M. Lutz and E. E. Kolomeitsev, Nucl. Phys. A **700**, 193 (2002)

[13] T. Hyodo, S. I. Nam, D. Jido and A. Hosaka, Phys. Rev. C **68**, 018201 (2003).

[14] E. Oset, A. Ramos and C. Bennhold, Phys. Lett. B **527**, 99 (2002). [Erratum-ibid. B **530**, 260 (2002)]

[15] C. Garcia-Recio, J. Nieves, E. Ruiz Arriola and M. J. Vicente Vacas, Phys. Rev. D **67**, 076009 (2003)

[16] D. Jido, J. A. Oller, E. Oset, A. Ramos and U. G. Meissner, Nucl. Phys. A **725**, 181 (2003).

[17] A. Ramos, E. Oset and C. Bennhold, Phys. Rev. Lett. **89**, 252001 (2002).

[18] C. Garcia-Recio, M. F. M. Lutz and J. Nieves, Phys. Lett. B **582**, 49 (2004).

[19] S. Prakhov *et al.* [Crystall Ball Collaboration], Phys. Rev. C **70**, 034605 (2004).

[20] V. K. Magas, E. Oset and A. Ramos, Phys. Rev. Lett. **95**, 052301 (2005).

[21] C. J. Batty, E. Friedman and A. Gal, Phys. Rept. **287**, 385 (1997).

[22] A. Baca, C. Garcia-Recio and J. Nieves, Nucl. Phys. A **673**, 335 (2000).

[23] V. Koch, Phys. Lett. B **337**, 7 (1994).

[24] T. Waas and W. Weise, Nucl. Phys. A **625**, 287 (1997) .

[25] M. Lutz, Phys. Lett. B **426**, 12 (1998).

[26] J. Schaffner-Bielich, V. Koch and M. Effenberger, Nucl. Phys. A **669**, 153 (2000).

[27] A. Ramos and E. Oset, Nucl. Phys. A **671**, 481 (2000).

[28] S. Hirenzaki, Y. Okumura, H. Toki, E. Oset and A. Ramos, Phys. Rev. C **61**, 055205 (2000).

[29] Y. Akaishi and T. Yamazaki, Phys. Rev. C **65**, 044005 (2002).

[30] E. Oset and H. Toki, arXiv:nucl-th/0509048.

[31] T. Suzuki *et al.*, Phys. Lett. B **597**, 263 (2004).

[32] Y. Akaishi, A. Dote and T. Yamazaki, Phys. Lett. B **613**, 140 (2005).

[33] M. Agnello *et al.* [FINUDA Collaboration], Phys. Rev. Lett. **94**, 212303 (2005).

[34] V. K. Magas, E. Oset, A. Ramos and H. Toki, arXiv:nucl-th/0601013.

[35] C. Garcia-Recio, E. Oset, A. Ramos and J. Nieves, Nucl. Phys. A **703**, 271 (2002).

[36] L. Tolos, A. Ramos, A. Polls and T. T. S. Kuo, Nucl. Phys. A **690**, 547 (2001).

[37] M. F. M. Lutz and C. L. Korpa, Nucl. Phys. A **700**, 309 (2002).

[38] D. Jido, E. Oset and A. Ramos, Phys. Rev. C **66**, 055203 (2002).

[39] J. A. Oller and E. Oset, Phys. Rev. D **60**, 074023 (1999).

[40] E. Oset and A. Ramos, Nucl. Phys. A **679**, 616 (2001).

[41] D. Cabrera and M. J. Vicente Vacas, Phys. Rev. C **67**, 045203 (2003).

[42] J. A. Oller, E. Oset and J. R. Pelaez, Phys. Rev. D **59**, 074001 (1999) [Erratum-ibid. D **60**, 099906 (1999)].

[43] M. Baldo, I. Bombaci, G. Giansiracusa, U. Lombardo, C. Mahaux and R. Sartor. Phys. Rev. C **41**, 1748 (1990).

[44] R. Brockmann and R. Machleidt, Phys. Rev. C **42**, 1965 (1990).

[45] D. J. Millener, C. B. Dover and A. Gal, Phys. Rev. C **38**, 2700 (1988).

[46] C. J. Batty, S. F. Biagi, M. Blecher, S. D. Hoath, R. A. J. Riddle, B. L. Roberts, J. D. Davies, G. J. Pyle, G. T. A. Squier and D. M. Asbury, Phys. Lett. B **74**, 27 (1978).

[47] C.J. Batty, Phys. Lett. B **87**, 324 (1979).

[48] A. Ramos, E. Oset and L. L. Salcedo, Phys. Rev. C **50**, 2314 (1994).

[49] A. B. Migdal, Rev. Mod. Phys. **50**, 107 (1978).

[50] C. Garcia-Recio, L. L. Salcedo and E. Oset, Phys. Rev. C **39**, 595 (1989).

[51] T. Hasegawa *et al.*, Phys. Rev. C **53**, 1210 (1996); P.H. Pile *et al.*, Phys. Rev. Lett. **66**, 2585 (1991); D.H. Davis, J.Pniewski, Contemp. Phys. **27**, 91 (1986); M. May *et al.*, Phys. Rev. Lett. **78**, 4343 (1997).

[52] A. Reuber, K. Holinde and J. Speth, Nucl. Phys. A **570**, 543 (1994).

[53] V. G. J. Stoks and Th. A. Rijken, Phys. Rev. C **59**, 3009 (1999); Th. A. Rijken, V. G. J. Stoks and Y. Yamamoto, Phys. Rev. C **59**, 21 (1999)

[54] I. Vidaña, A. Polls, A. Ramos and H. J. Schulze, Phys. Rev. C **64**, 044301 (2001).

[55] J. Haidenbauer and Ulf-G. Meissner, Phys. Rev. C **72**, 044005 (2005).

[56] M. Kaskulov and E. Oset, arXiv:nucl-th/0509088.

[57] E. Oset, P. Fernandez de Cordoba, L. L. Salcedo and R. Brockmann, Phys. Rept. **188**, 79 (1990).

[58] C. J. Batty, E. Friedman and A. Gal, Phys. Lett. B **335**, 273 (1994).

[59] J. Mares, E. Friedman, A. Gal and B. K. Jennings, Nucl. Phys. A **594**, 311 (1995).

[60] N. Kaiser, Phys. Rev. C **71**, 068201 (2005).

[61] H. Noumi *et al.*, Phys. Rev. Lett. **89**, 072301 (2002) [Erratum-ibid. **90** (2003) 049902].

[62] P. K. Saha *et al.*, Phys. Rev. C **70**, 044613 (2004).

[63] M. Kohno, Y. Fujiwara, Y. Watanabe, K. Ogata and M. Kawai, Prog. Theor. Phys. **112**, 895 (2004).

[64] O. Morimatsu and K. Yazaki, Prog. Part. Nucl. Phys. **33**, 679 (1994).

[65] J. Nieves, E. Oset and C. Garcia-Recio, Nucl. Phys. A **554**, 554 (1993) .

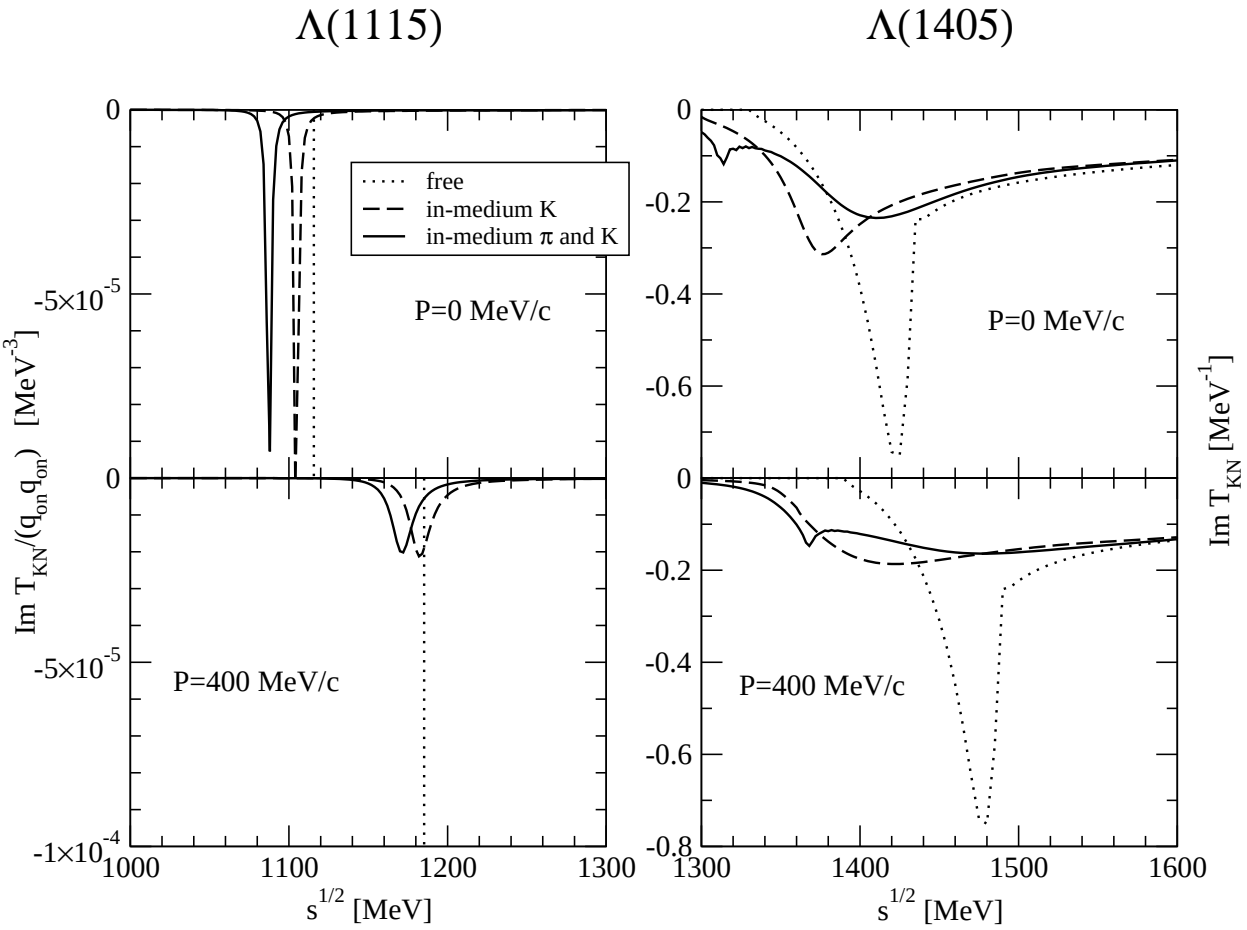

FIG. 7: Imaginary part of the I=0, J^P=1/2$^+$, $\bar{K}N \to \bar{K}N$ amplitude as a function of $\sqrt{s}$ for two values of the momentum $\mid \vec{P} \mid$, in the s- (right panel) and p- (left panel) waves. The free space amplitudes (dotted lines) are compared with the in-medium amplitude at ρ=ρ_0 dressing only antikaons (dashed lines) or dressing also the pions (solid lines).

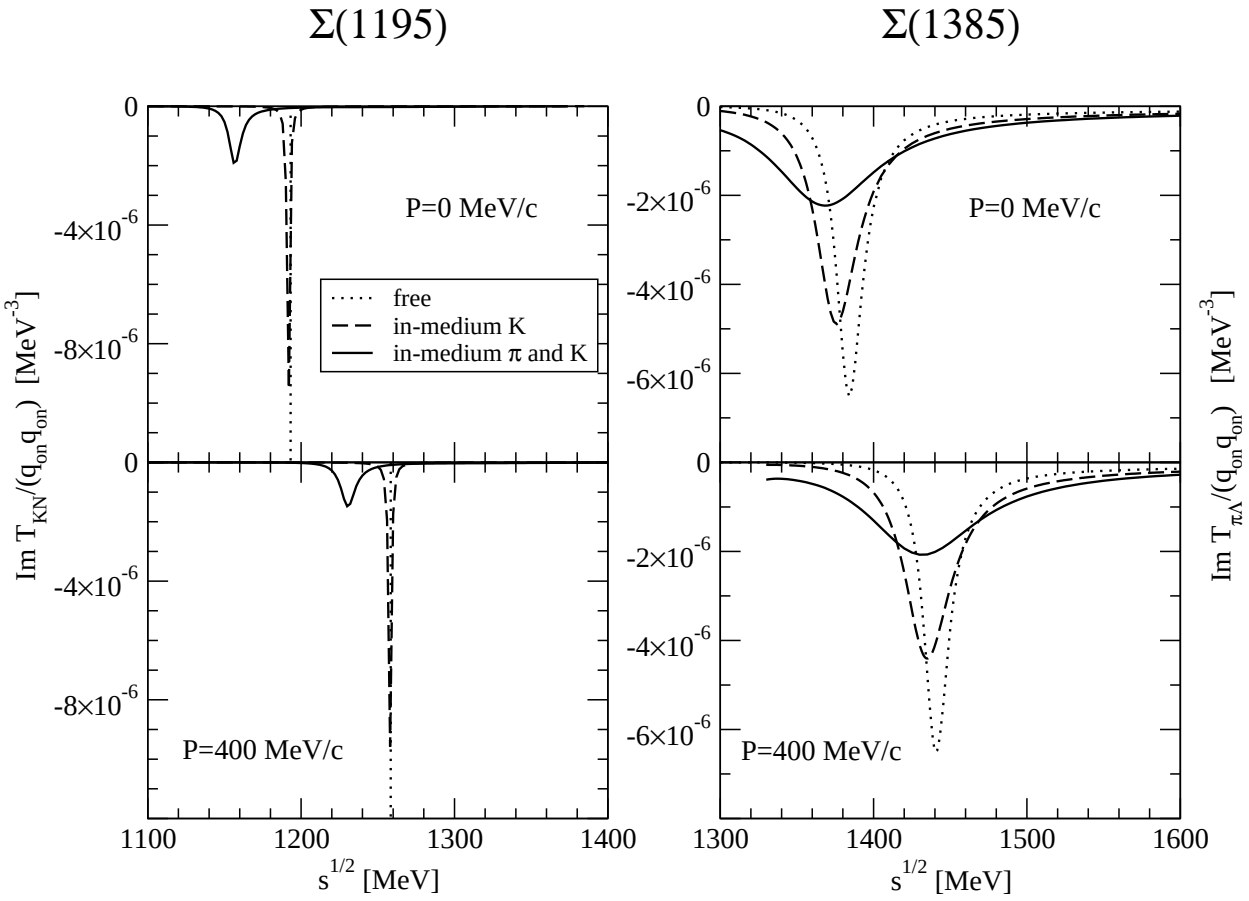

FIG. 8: Imaginary part of the I=1, J^P=1/2$^+$, L=1 $\bar{K}N \to \bar{K}N$ amplitude and of the I=1, J^P=3/2$^+$, L=1 $\pi\Lambda \to \pi\Lambda$ amplitude as functions of $\sqrt{s}$ for two values of the momentum $\mid \vec{P} \mid$. The free space amplitudes (dotted lines) are compared with the in-medium amplitudes at ρ=ρ_0 dressing only antikaons (dashed lines) or dressing also the pions (solid lines).

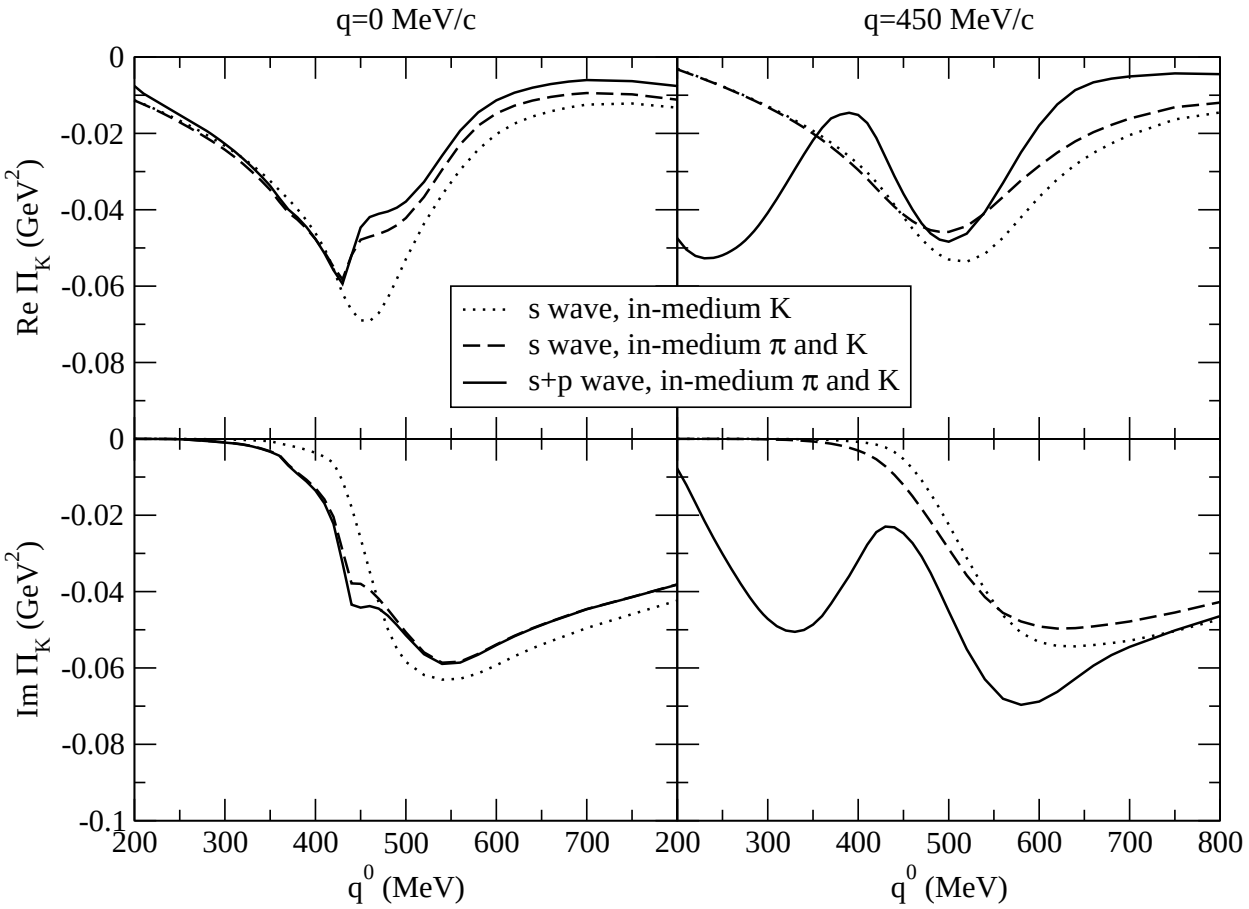

FIG. 9: Real part (upper panels) and imaginary part (lower panels) of the antikaon self-energy as functions of the antikaon energy q^0, for two values of the antikaon momentum, $q = 0$ MeV/c (left panels) and $q = 450$ MeV/c (right panels).

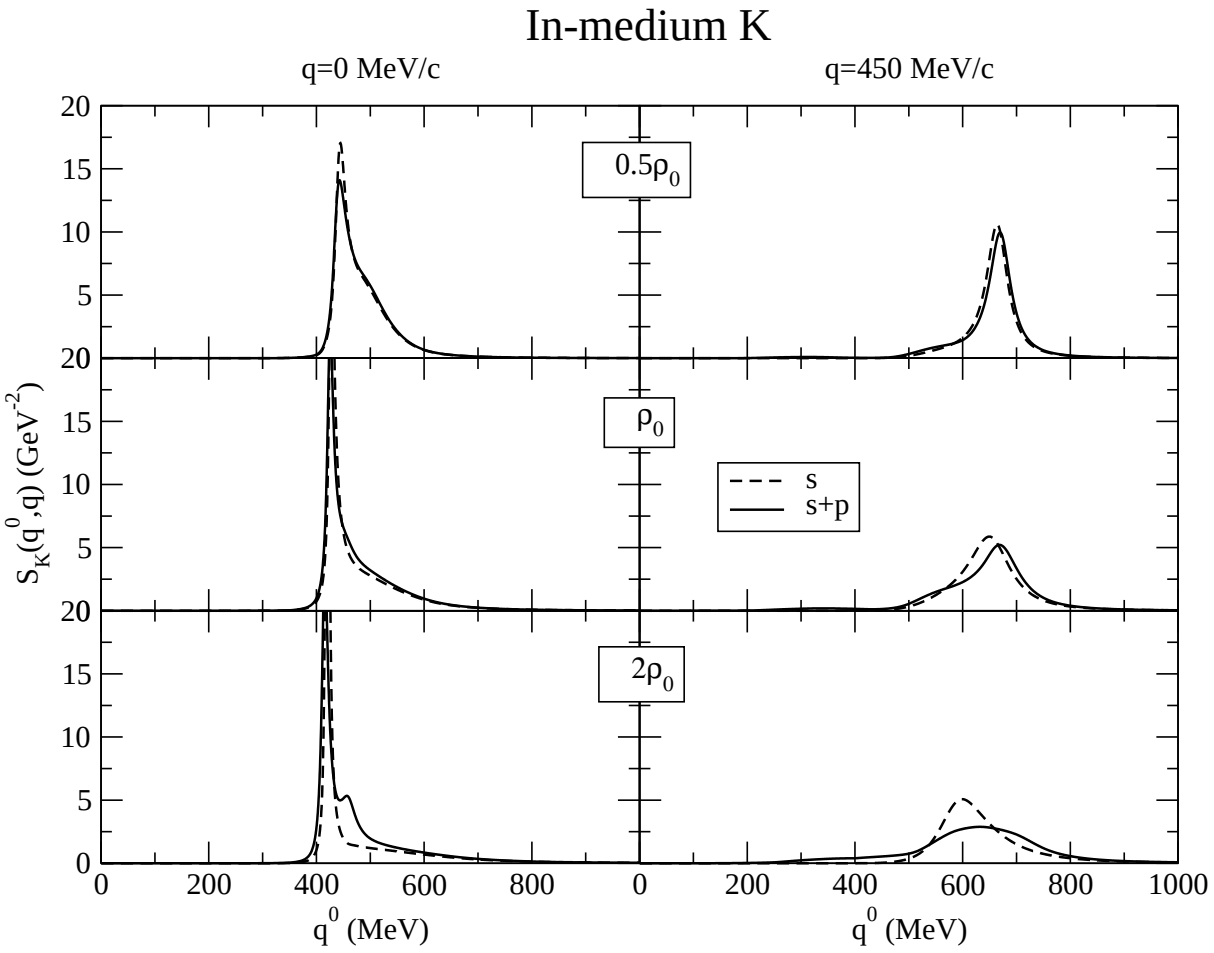

FIG. 10: Antikaon spectral function as a function of the antikaon energy q^0, for two values of the antikaon momentum, $q = 0$ MeV/c (left panels) and $q = 450$ MeV/c (right panels), and three values of density, ρ=0.5ρ_0, ρ_0 and 2ρ_0. These results have been obtained for the approximation in which only the antikaons are dressed self-consistently.

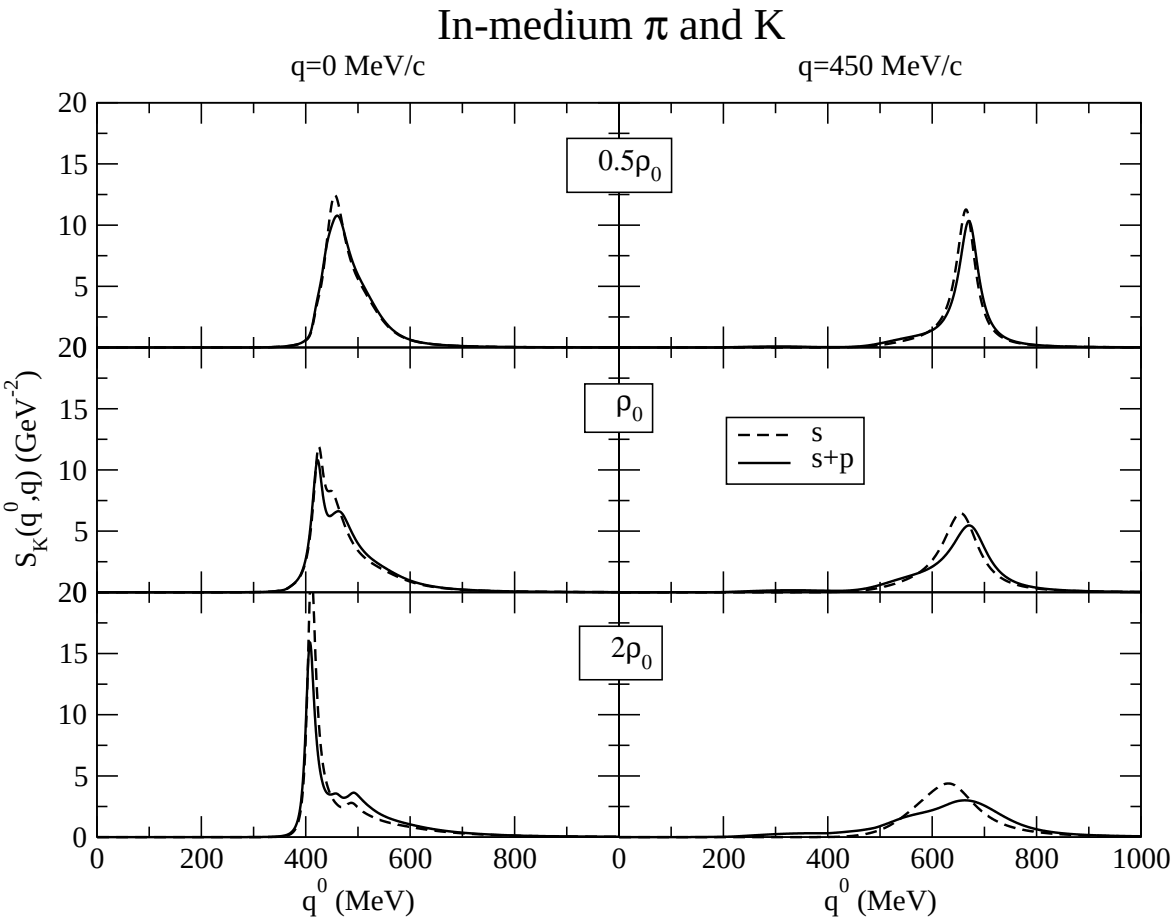

FIG. 11: The same as Fig. 10 but with the approximation that also considers the dressing of the pions.

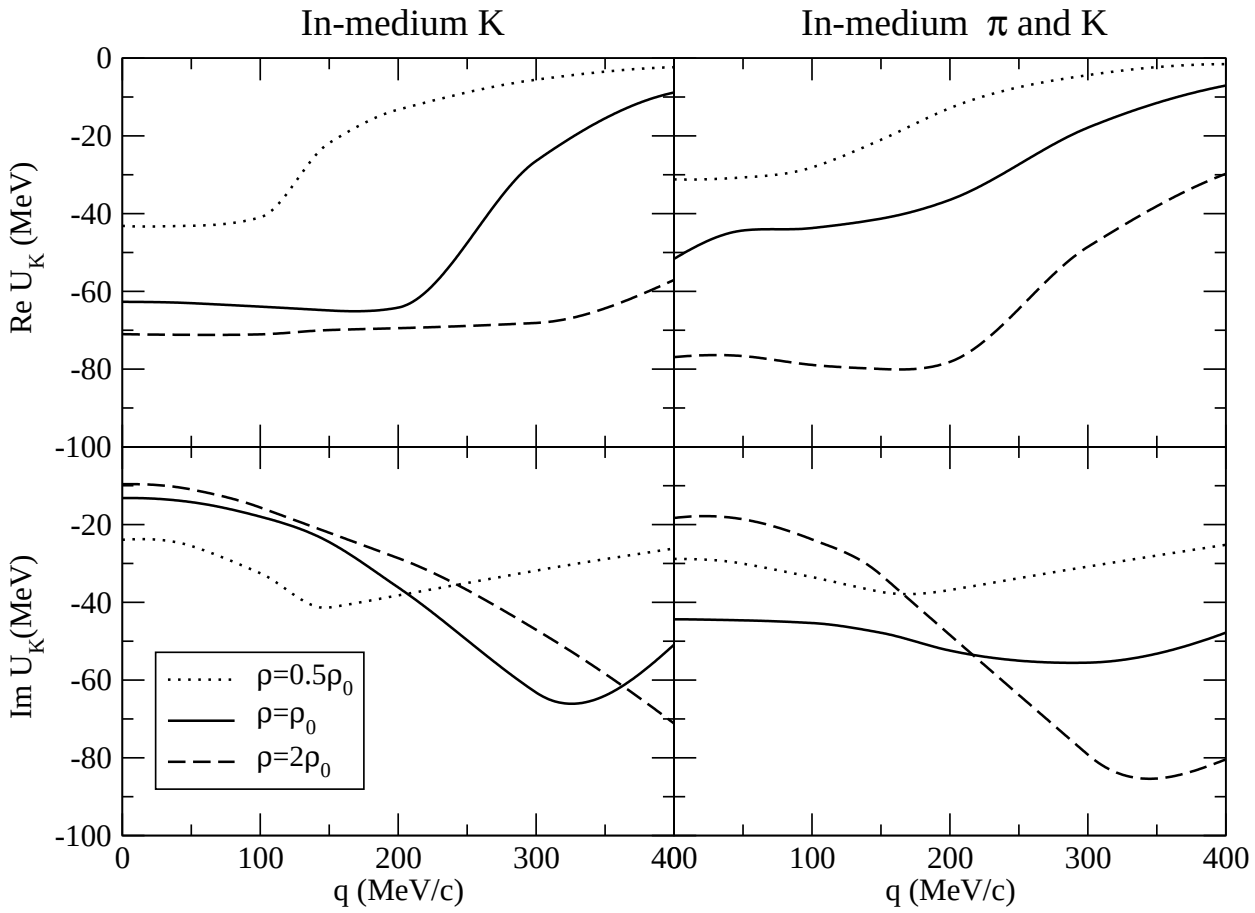

FIG. 12: Real part (upper panels) and imaginary part (lower panels) of the antikaon optical potential as functions of the antikaon momentum for three values of density, ρ=0.5ρ_0, ρ_0 and 2ρ_0 and two approximations, dressing only kaons (left panels) and dressing also the pions (right panels).